crystals

MDPI

Article

Novel Method for Estimating Phosphor Conversion Efficiency of Light-Emitting Diodes

Chih-Hao Lin [1], Che-Hsuan Huang [1], Yung-Min Pai [1], Chung-Fu Lee [1], Chien-Chung Lin [2], Chia-Wei Sun [1], Cheng-Huan Chen [1], Chin-Wei Sher [1,3,*] and Hao-Chung Kuo [1,*]

1 Department of Photonics and Institute of Electro-Optical Engineering, National Chiao Tung University, Hsinchu 30010, Taiwan; actupon@gmail.com (C.-H.L.); seadeep08281226@gmail.com (C.-H.H.); f926202@gmail.com (Y.-M.P.); ian.727@gmail.com (C.-F.L.); chiaweisun@nctu.edu.tw (C.-W.S.); chhuchen@nctu.edu.tw (C.-H.C.)

2 Institute of Photonic System, National Chiao Tung University, Tainan 711, Taiwan; chienchunglin@faculty.nctu.edu.tw

3 Fok Ying Tung Research Institute, Hong Kong University of Science and Technology, Hong Kong 511458, China

* Correspondence: steven.sher@hotmail.com (C.-W.S.); hckuo@faculty.nctu.edu.tw (H.-C.K.)

Received: 23 October 2018; Accepted: 26 November 2018; Published: 27 November 2018

Abstract: This study presents a novel method for estimating the phosphor conversion efficiency of white light-emitting diodes (WLEDs) with different ratios of phosphors. Numerous attempts have been made for predicting the phosphor conversion efficiency of WLEDs using Monte Carlo ray tracing and the Mie scattering theory. However, because efficiency depends on the phosphor concentration, obtaining a tight match between this model and the experimental results remains a major challenge. An accurate prediction depends on various parameters, including particle size, morphology, and packaging process criteria. Therefore, we developed an efficient model that can successfully correlate the total absorption ratio to the phosphor concentration using a simple equation for estimating the spectra and lumen output. The novel and efficient method proposed here can accelerate WLED development by reducing costs and saving fabrication time.

Keywords: light emitting diode; electro-optical devices

1. Introduction

Recently, light-emitting diodes (LEDs) have gained considerable attention because of their long-lifetime, high-efficiency, and energy-saving properties which make them good candidates for solid-state lighting [1–3]. White LEDs (WLEDs) through epitaxy using GaN-based chips have demonstrated great improvements in efficiency [4–8]. The basic concept underlying WLED fabrication involves coating blue LEDs (BLEDs) with a yellow light-emitting color-conversion element, such as phosphors or organic dyes. This has become the most common approach for white light generation [9]. To achieve different color gamut, color rendering index (CRI), light quality, and efficiency specifications for various applications, many novel phosphors that increase the efficiency or color performance of LEDs have been developed [10–13]. Among the several phosphors for LED applications, yttrium aluminum garnet (YAG)-, silicate-, and nitride-based phosphors are used most widely in WLEDs because of their well developed fabrication processes and outstanding features. Several studies have focused on optimizing the package design of LEDs to improve their efficiency and color quality. The parameters of the LED packaging depend on the type of phosphor and dopant concentration used. These properties considerably affect the LEDs' efficiency, correlated color temperature (CCT), and CRI [14–17]. For practical applications, simulating the spectrum or chromatic performance of LEDs

under various design conditions is necessary. Many researchers have investigated models based on Monte Carlo ray tracing combined with the Mie scattering theory [18–23]. However, accurate prediction results have been difficult to achieve, regardless of the parameters used, including the absorption coefficient, particle size distribution, phosphor density, scattering model, and phosphor morphology. Numerous attempts to develop an accurate simulation platform have provided suboptimal results, thereby indicating that accurate simulation requires substantial effort and experience because the microscope properties of phosphor are unavoidable for accurate simulation [24–28]. Despite these efforts, predicting the spectrum precisely when the package design or type of phosphor changes in real cases remains difficult. Different phosphors have different crystal phases, particle size distributions, and morphologies, which are hard to measured and define specifications for. The phosphor particle size distribution and morphology are the main factors affecting the accuracy of a simulation model. However, even when all the essential information from the emitting materials is measured to predict the performance of WLEDs, the simulation remains restricted to a narrow range, such as single-package geometry, as well as the fixed physical properties of phosphor. Therefore, this paper presents a novel method based on a wavelength conversion concept instead of a traditional complex simulation in order to increase the consistency between predicted results and experimental data. The proposed wavelength conversion method is more suitable than microcosmic concepts involving complicated scattering cases, which lead to unpredictable simulation results.

A novel method based on the down-conversion luminescence efficiency (DCLE) concept is employed to predict the performance of the LED, including the pumping source and emitted photons for any package design. The major difference between this model and traditional simulations is that it is easier to measure the parameters required when using out method, and it is more straightforward to correlate the total absorption ratio to the phosphor concentration in real applications. We believe that this method will accelerate the development of WLED applications because of its simplicity, high accuracy, and lack of rigorous restrictions.

2. DCLE Concept for Phosphor Conversion System

Figure 1 is the schematic of a WLED used for the novel model in this study. A dispensing package was used as the template. In general, the white light emitted by a WLED comprises blue photons and fluorescent yellow rays emitted from the phosphor. Here, the white light was divided into two parts to analyze the wavelength conversion between the BLEDs and the phosphors. The algorithm for the phosphor conversion system was developed by analyzing the wavelength conversion between the two parts in an emission spectrum of white light.

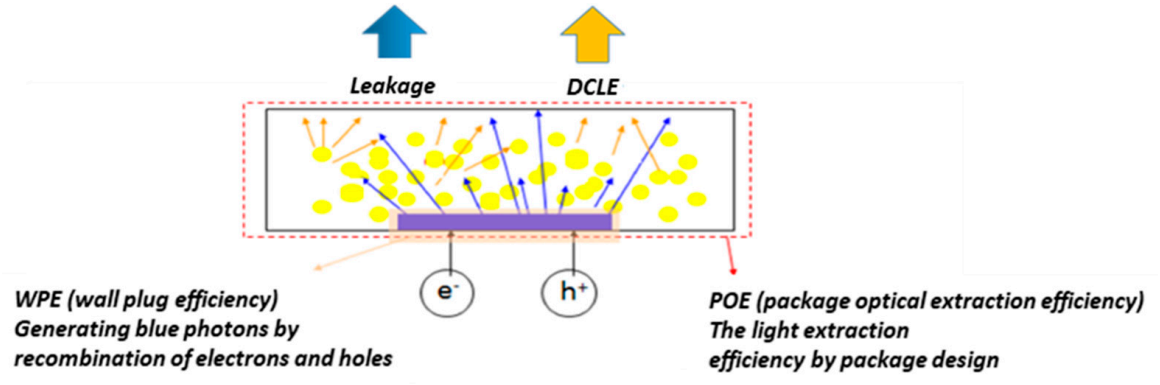

Figure 1. Schematic of a WLED structure.

3. Phosphor Conversion Model Based on the DCLE Concept

To develop an optical model of the WLED, the DCLE mechanism was identified as a phenomenological approach. Where I is the fraction of leakage from the pumping light source

(blue rays) and $P_{B\text{-}LED}$ is the radiant flux of the BLED in the package. Hence, the down-converted light could be reformulated and written as follows:

$$\text{Down} - \text{converted light} = (1 - I) \times P_{B-LED} \times E_{\lambda p-\lambda ph1,PKG} \quad (1)$$

where $E_{\lambda p-\lambda ph1,PKG}$ represents the extraction efficiencies of blue light, emission light, and the material.

All calculations were performed according to the flowchart in Figure 2. First, two samples were prepared: A BLED without phosphor coating and a BLED with phosphor coating (i.e., a WLED).

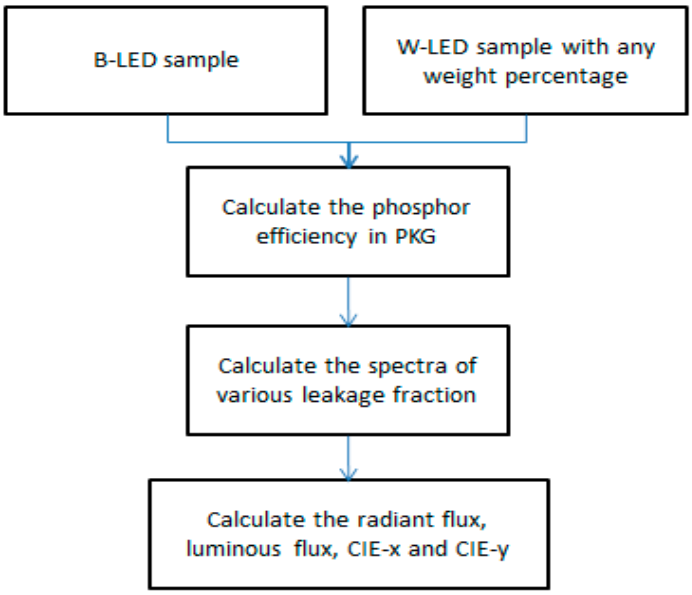

Figure 2. Flowchart of the singular phosphor model.

The spectrum of the BLEDs where no light conversion (I = 1) occurs, indicates a radiant flux of approximately 74 mW, as illustrated in Figure 3a. Figure 3b shows the emission spectrum under total conversion for the WLED (I = 0). The radiant flux was approximately 66 mW and all the blue light was absorbed. The efficiency $E_{\lambda p-\lambda ph1,PKG}$ was calculated by dividing the radiant flux of the WLED by the difference in absorption powers of BLED and WLED, which was 0.72 (= 53.28/74).

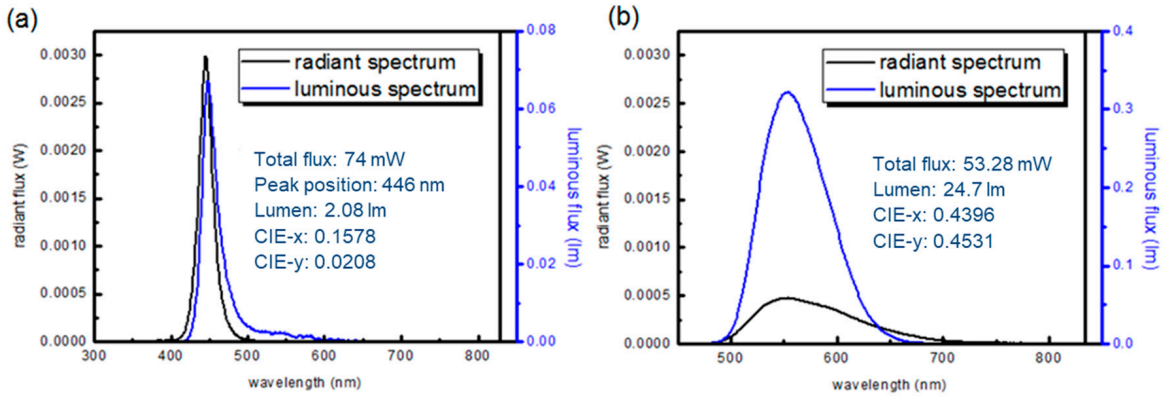

Figure 3. Spectra of leaked blue rays: (**a**) I = 1 (only blue light) and (**b**) I = 0 (no blue light).

Next, the value of the leakage fraction I was varied by changing the blue-to-white-light ratio. The spectra simulated according to the DCLE theorem can be used to calculate the CIE1931 coordinate and the luminous flux. Figure 4 shows the calculation results for different I values.

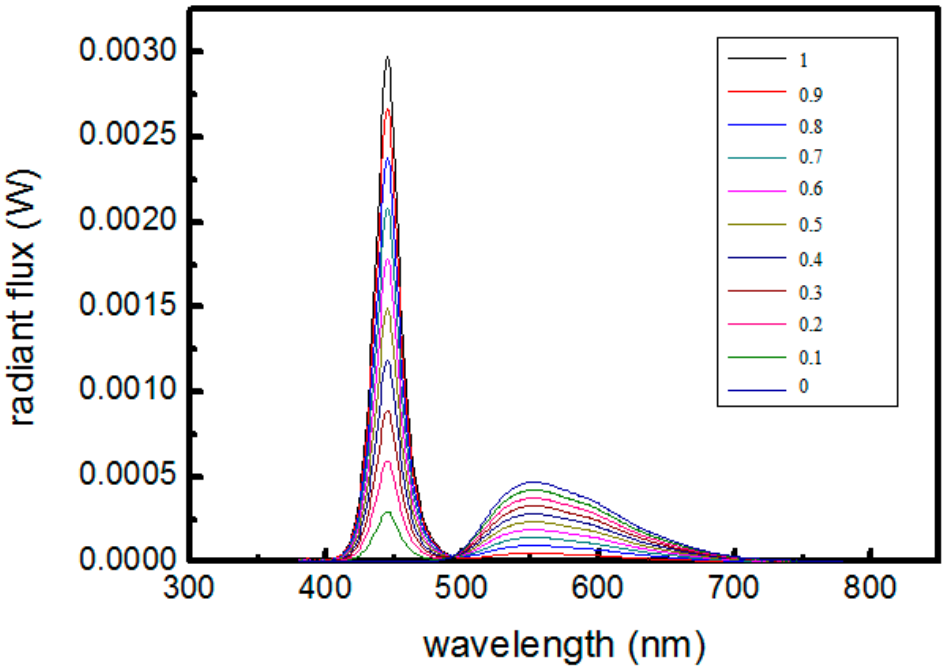

Figure 4. Calculated results for different leakage fractions.

Table 1 presents the calculation results for different leakage fractions. The distribution of the visual function shows that human eyes are more sensitive at 550 nm; thus, one part of the emission spectrum accounts for a predominant portion of the luminous flux. The more energy the part emits, the higher the value of luminous flux is. This type of wavelength conversion also leads to higher values of color coordinates.

Table 1. Calculated results for different leakage fractions.

Leakage Fraction	0	0.1	0.2	0.3	0.4	0.5	0.6	0.7	0.8	0.9	1
Radiant Flux (mW)	53.3	55.4	57.4	59.5	61.6	63.6	65.7	67.78	69.9	72	74
Luminous Flux (lm)	24.7	22.5	20.2	17.9	15.7	13.4	11.1	8.9	6.6	4.3	2.1
CIE-x	0.439	0.384	0.340	0.304	0.273	0.247	0.224	0.204	0.167	0.172	0.158
CIE-y	0.543	0.441	0.359	0.291	0.234	0.186	0.143	0.107	0.075	0.046	0.021

To verify the precision of the DCLE concept of phosphor conversion in the LED package, we investigated the relationship between the calculation and experimental results at various phosphor concentrations. We applied a surface-mounted device (SMD) type 3030 (3.0 × 3.0 mm^2) LED, with a configuration consisting of 22 × 35-mil blue die operating at 60 mA (Lextar Electronics Corporation, Hsinchu, Taiwan); a YAG phosphor mixture (NYAG4 from Intematix, CA, USA) was used in varying concentrations from 10% to 50%. Optical measurements were performed using a spectrometer: CAS 140CT (Instrument System GmbH, Munich, Germany), with a 50-cm integrating sphere and 0.5 nm resolution. Figure 5 demonstrates that the luminous flux depends on the leakage fraction. Our results demonstrated a high linear correlation under 50% concentration and a low junction temperature of <60 °C. It therefore should carefully control the LED package design to avoid concentration quench and phosphor thermal quench as not to cause a failed prediction. According to our past experiences, the leakage ratio should be not lower than 0.2 as not to cause concentration quench in a normal case, and lower junction temperature of <100 °C for the most commonly used materials such as YAG and red nitride phosphor in lighting applications. Therefore, DCLE could be a favorable concept for application without difficult-to-measure parameters or any limitation on the package or phosphor type used. Moreover, the target CIE coordination of the LED package for different applications depends on the phosphor concentration applied in real cases. Hence, we derived the following equations based on

the weight percentage of the phosphor, instead of the leakage fraction. We used the total absorption ratio A_t, (which is equal to 1 − leakage fraction (I)) for the subsequent model derivation.

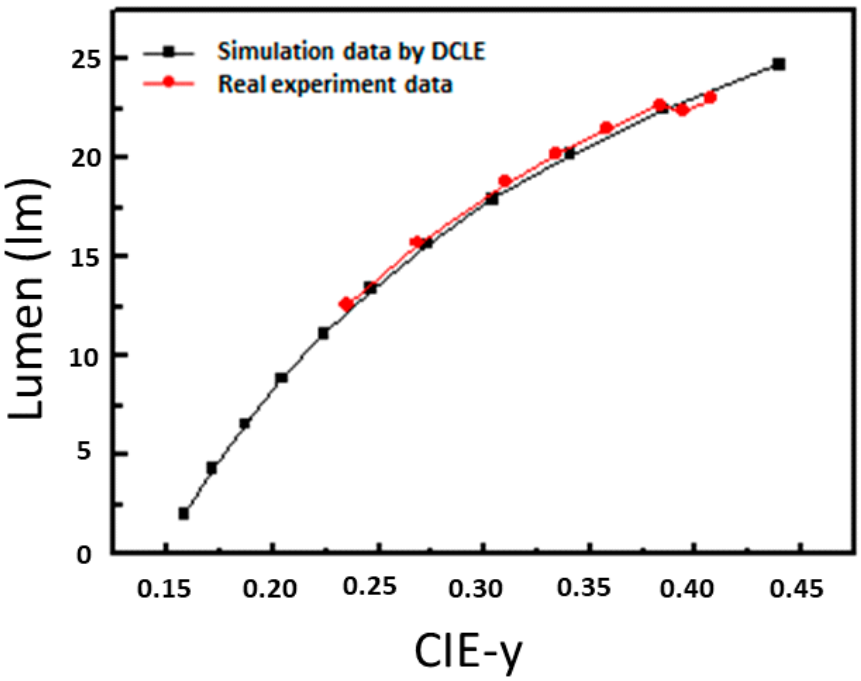

Figure 5. Simulation and experimental results.

4. Novel Model for Phosphor Wavelength Conversion

In the proposed absorption model, the total absorption ratio A_t can be written as:

$$\text{Total absorption ratio}(A_t) = \left[1 - A_{system}(1 - A)^n\right] \quad (2)$$

where A is the absorption ratio of each particle from the emission material and n is the statistical mean average number of absorption processes that the LED beam undergoes inside the phosphor material. In addition to these parameters, the absorption curve is affected by the LED package; consequently, the fixed term A_{system} is added to Equation (2). To analyze the parameters of the absorption curve, Equation (2) can be rewritten as follows:

$$\ln(1 - A_t) = n \ln(1 - A) + \ln A_{system} \quad (3)$$

here, n is a key parameter supposed to be highly related to the weight index w, which represents the total weight of the phosphor grains. Because the greater the phosphor quantity, the higher the excitation possibility. For the purpose of performing this calculation, an assumption of the excitation model is presented in Equation (4). The excitation times of phosphor n is affected by the optic length (OL) and the probability of pumping. The OL depends on the packaging system used, and the probability of pumping is related to the sum of the volume of the phosphor v within the system volume V. It is also proportional to the surface area of the phosphor, and hence, the fixed term $4\pi r^2 / \left(\frac{4}{3}\pi r^3\right)$ is added to Equation (4):

$$n \propto OL \cdot (v/V) \cdot 4\pi r^2 / \left(\frac{4}{3}\pi r^3\right) \quad (4)$$

where the effective radius of the phosphor $r = (3v/4N\pi)^{1/3}$ and the parameter N is the number of phosphor particles. Then, Equation (4) can be arranged as Equations (5) and (6):

$$n \propto OL \cdot (v/V) \cdot (3/r) \tag{5}$$

$$n = Cw^{\frac{2}{3}} \tag{6}$$

where the coefficient C includes OL, N, V, d, and other geometric terms, and d and w represent the density and total weight of the phosphor, respectively. Equation (3) can then be written as follows:

$$\ln(1 - A_t) = Cw^{\frac{2}{3}} \ln(1 - A) + \ln A_{system} \tag{7}$$

The important parameters in the preceding equation are A_t and w, which is the total weight of phosphor. To simplify the equation, the parameters C and $(1 - A)$ are combined as C'. This equation can be split into Equations (8) and (9).

$$\ln(1 - A_t) = C'w^{\frac{2}{3}} + \ln A_{system} \tag{8}$$

$$A_t = 1 - \exp\left[C'w^{\frac{2}{3}} + \ln A_{system}\right] \tag{9}$$

We performed experiments by packaging yellow YAG and silicate phosphor in an LED package and measuring the real A_t values to verify our proposed model. We used the aforementioned SMD from Lextar Electronic along with YAG and silicate phosphor mixture (NYAG4 and Y4453 from Intematix, Fremont, CA, USA) and silicone resin (6631; Dowcorning, Midland, MI, USA). The emission peak and particle size were respectively 560 nm and 15 μm for YAG and 563 nm and 20 μm for silicate phosphor. Equation (9) can be used to predict A_t in terms of weight percentage. To prove the preceding assumption, we performed experiments using the various values listed in Table 2.

Table 2. Absorption coefficients of YAG and silicate phosphors in a real package.

Material	**YAG**		**Silicate**	
w (%)	**A_t**	**ln(A_t)**	**A_t**	**ln(A_t)**
10%	14%	−1.9661	9.86%	−2.3166
15%	14.6%	−1.9241	13.4%	−2.2164
20%	15.3%	−1.8770	12.51%	−2.0786
25%	15.8%	−1.8451	12.51%	−2.0010
30%	16.26%	−1.8159	14.71%	−1.9167

Figure 6 shows that the coefficients of determination (R squared) are 99.68% for YAG and 99.65% for silicate in the 3030 LED package, which demonstrated a strong linear relationship between $\ln A_t$ and $w^{2/3}$. These real packaging data, regardless of whether it was YAG or silicate phosphor, fulfilled the aforementioned proposed model. Thus, according to this novel method, a precise phosphor conversion system is feasible.

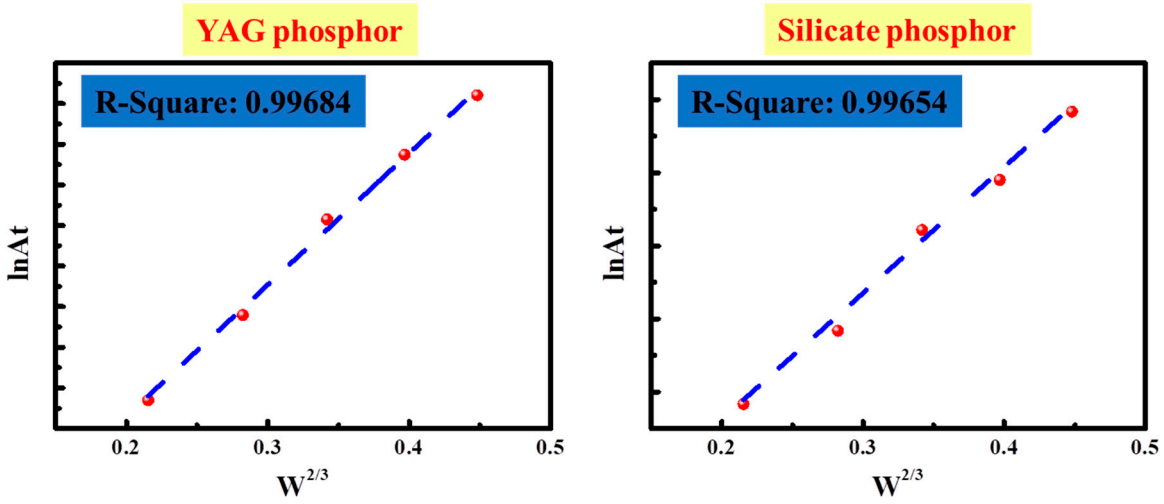

Figure 6. $\ln A_t$ versus $W^{2/3}$ for YAG and silicate phosphors in real package.

5. Conclusions

This paper presented a method for calculating phosphor conversion efficiency from the viewpoint of wavelength conversion. Our proposed algorithm successfully correlates the total absorption ratio A_t to the phosphor concentration and thus can accurately predict the efficacy and spectrum even for different phosphor types with random sizes and morphologies. In this work, an algorithm was used to derive a simple equation for estimating the spectra and lumen output of silicate and YAG phosphors in the same package by varying their concentrations. The use of only YAG or only silicate phosphor, typically results in cool white light with relatively high CCT and poor CRI, which reflects their application in room WLED-used lighting. Therefore, various Mn4+- doped fluoride/oxide narrow-band red-emitting phosphors have been extensively studied for their high photoluminescence quantum yields, exhibiting broadband absorption in the blue region and narrow-band emission in the red spectral region [29]. By applying the model discussed in this paper, it is also possible to accurately simulate phosphor conversion efficiency of "warm" WLEDs with the addition of a red-emitting phosphor to YAG/silicate yellow phosphor. We believe that our novel and efficient method can accelerate the development of many novel luminescent materials in different design packages.

Author Contributions: Data curation, C.-H.L.; Formal analysis, C.-H.H.; Investigation, C.-H.L. and Y.-M.P.; Methodology, Y.-M.P.; Resources, C.-F.L.; Software, C.-H.H.; Supervision, C.-C.L., C.-W.S. (Chia-Wei Sun), C.-H.C. and C.-W.S. (Chin-Wei Sher); Writing—original draft, C.-H.L.; Writing—review & editing, H.-C.K.

Funding: This research was funded by the Ministry of Science and Technology of Taiwan through grant numbers MOST107-2221-E-009-113-MY3 and MOST106-2622-E-009-005-CC2.

Acknowledgments: The authors express their gratitude to Lextar Corporation and LEDA-creative Corporation for their technical support and helpful discussion.

Conflicts of Interest: The authors declare no conflict of interest.

References

1. Pimputkar, S.; Speck, J.S.; DenBaars, S.P.; Nakamura, S. Prospects for LED lighting. *Nat. Photonics* **2009**, *3*, 180. [CrossRef]
2. Amano, H.; Kito, M.; Hiramatsu, K.; Akasaki, I. P-type conduction in Mg-doped GaN treated with low-energy electron beam irradiation (LEEBI). *Jpn. J. Appl. Phys.* **1989**, *28*, L2112. [CrossRef]
3. Schubert, E.F.; Kim, J.K. Solid-state light sources getting smart. *Science* **2005**, *308*, 1274–1278. [CrossRef] [PubMed]
4. Lin, C.C.; Liu, R.-S. Advances in phosphors for light-emitting diodes. *J. Phys. Chem. Lett.* **2011**, *2*, 1268–1277. [CrossRef] [PubMed]

5. Nakamura, S.; Mukai, T.; Senoh, M. Candela-class high-brightness InGaN/AlGaN double-heterostructure blue-light-emitting diodes. *Appl. Phys. Lett.* **1994**, *64*, 1687–1689. [CrossRef]
6. Nakamura, S.; Senoh, M.; Iwasa, N.; Nagahama, S.-i. High-power InGaN single-quantum-well-structure blue and violet light-emitting diodes. *Appl. Phys. Lett.* **1995**, *67*, 1868–1870. [CrossRef]
7. Huang, H.-W.; Kao, C.; Chu, J.; Kuo, H.; Wang, S.; Yu, C. Improvement of InGaN-GaN light-emitting diode performance with a nano-roughened p-GaN surface. *IEEE Photon. Technol. Lett.* **2005**, *17*, 983–985. [CrossRef]
8. Ling, S.-C.; Lu, T.-C.; Chang, S.-P.; Chen, J.-R.; Kuo, H.-C.; Wang, S.-C. Low efficiency droop in blue-green m-plane InGaN/GaN light emitting diodes. *Appl. Phys. Lett.* **2010**, *96*, 231101. [CrossRef]
9. Krames, M.R.; Shchekin, O.B.; Mueller-Mach, R.; Mueller, G.O.; Zhou, L.; Harbers, G.; Craford, M.G. Status and future of high-power light-emitting diodes for solid-state lighting. *J. Disp. Technol.* **2007**, *3*, 160–175. [CrossRef]
10. Liu, C.-Y.; Chen, K.-J.; Lin, D.-W.; Lee, C.-Y.; Lin, C.-C.; Chien, S.-H.; Shih, M.-H.; Chi, G.-C.; Chang, C.-Y.; Kuo, H.-C. Improvement of emission uniformity by using micro-cone patterned PDMS film. *Opt. Express* **2014**, *22*, 4516–4522. [CrossRef] [PubMed]
11. Lin, H.-Y.; Chen, K.-J.; Wang, S.-W.; Lin, C.-C.; Wang, K.-Y.; Li, J.-R.; Lee, P.-T.; Shih, M.-H.; Li, X.; Chen, H.-M. Improvement of light quality by DBR structure in white LED. *Opt. Express* **2015**, *23*, A27–A33. [CrossRef] [PubMed]
12. Chen, H.C.; Chen, K.J.; Wang, C.H.; Lin, C.C.; Yeh, C.C.; Tsai, H.H.; Shih, M.H.; Kuo, H.C.; Lu, T.C. A novel randomly textured phosphor structure for highly efficient white light-emitting diodes. *Nanoscale Res. Lett.* **2012**, *7*, 188. [CrossRef] [PubMed]
13. Kuo, H.-C.; Hung, C.-W.; Chen, H.-C.; Chen, K.-J.; Wang, C.-H.; Sher, C.-W.; Yeh, C.-C.; Lin, C.-C.; Chen, C.-H.; Cheng, Y.-J. Patterned structure of remote phosphor for phosphor-converted white LEDs. *Opt. Express* **2011**, *19*, A930–A936. [CrossRef] [PubMed]
14. Lin, H.-Y.; Wang, S.-W.; Lin, C.-C.; Chen, K.-J.; Han, H.-V.; Tu, Z.-Y.; Tu, H.-H.; Chen, T.-M.; Shih, M.-H.; Lee, P.-T. Excellent color quality of white-light-emitting diodes by embedding quantum dots in polymers material. *IEEE J. Sel. Top. Quant. Electron.* **2016**, *22*, 35–41. [CrossRef]
15. Lin, H.-Y.; Sher, C.-W.; Lin, C.-H.; Tu, H.-H.; Chen, X.Y.; Lai, Y.-C.; Lin, C.-C.; Chen, H.-M.; Yu, P.; Meng, H.-F. Fabrication of Flexible White Light-Emitting Diodes from Photoluminescent Polymer Materials with Excellent Color Quality. *ACS Appl. Mater. Interfaces* **2017**, *9*, 35279–35286. [CrossRef] [PubMed]
16. Sher, C.-W.; Lin, C.-H.; Lin, H.-Y.; Lin, C.-C.; Huang, C.-H.; Chen, K.-J.; Li, J.-R.; Wang, K.-Y.; Tu, H.-H.; Fu, C.-C. A high quality liquid-type quantum dot white light-emitting diode. *Nanoscale* **2015**, *8*, 1117–1122. [CrossRef] [PubMed]
17. Sher, C.-W.; Chen, K.-J.; Lin, C.-C.; Han, H.-V.; Lin, H.-Y.; Tu, Z.-Y.; Tu, H.-H.; Honjo, K.; Jiang, H.-Y.; Ou, S.-L. Large-area, uniform white light LED source on a flexible substrate. *Opt. Express* **2015**, *23*, A1167–A1178. [CrossRef] [PubMed]
18. Lee, S.J. Analysis of light-emitting diodes by Monte Carlo photon simulation. *Appl. Opt.* **2001**, *40*, 1427–1437. [CrossRef] [PubMed]
19. Sommer, C.; Reil, F.; Krenn, J.R.; Hartmann, P.; Pachler, P.; Tasch, S.; Wenzl, F.P. The impact of inhomogeneities in the phosphor distribution on the device performance of phosphor-converted high-power white LED light sources. *J. Light. Technol.* **2010**, *28*, 3226–3232. [CrossRef]
20. Ting, D.Z.; McGill, T.C. Monte Carlo simulation of light-emitting diode light-extraction characteristics. *Opt. Eng.* **1995**, *34*, 3545–3554. [CrossRef]
21. Borbély, Á.; Johnson, S.G. Performance of phosphor-coated light-emitting diode optics in ray-trace simulations. *Opt. Eng.* **2005**, *44*, 111308. [CrossRef]
22. Liu, Z.; Wang, K.; Luo, X.; Liu, S. Precise optical modeling of blue light-emitting diodes by Monte Carlo ray-tracing. *Opt. Express* **2010**, *18*, 9398–9412. [CrossRef] [PubMed]
23. Liu, Z.-Y.; Liu, S.; Wang, K.; Luo, X.-B. Studies on optical consistency of white LEDs affected by phosphor thickness and concentration using optical simulation. *IEEE Trans. Compon. Packag. Technol.* **2010**, *33*, 680–687. [CrossRef]
24. Yang, T.-H.; Chen, C.-C.; Chen, C.-Y.; Chang, Y.-Y.; Sun, C.-C. Essential factor for determining optical output of phosphor-converted LEDs. *IEEE Photon. J.* **2014**, *6*, 1–9. [CrossRef]
25. Kang, D.-Y.; Wu, E.; Wang, D.-M. Modeling white light-emitting diodes with phosphor layers. *Appl. Phys. Lett.* **2006**, *89*, 231102. [CrossRef]

26. Sun, C.-C.; Chen, C.-Y.; He, H.-Y.; Chen, C.-C.; Chien, W.-T.; Lee, T.-X.; Yang, T.-H. Precise optical modeling for silicate-based white LEDs. *Opt. Express* **2008**, *16*, 20060–20066. [CrossRef] [PubMed]
27. Yang, T.-H.; Chen, C.-Y.; Chang, Y.-Y.; Glorieux, B.; Peng, Y.-N.; Chen, H.-X.; Chung, T.-Y.; Lee, T.-X.; Sun, C.-C. Precise simulation of spectrum for green emitting phosphors pumped by a blue LED die. *IEEE Photon. J.* **2014**, *6*, 1–10.
28. Sommer, C.; Wenzl, F.-P.; Hartmann, P.; Pachler, P.; Schweighart, M.; Tasch, S.; Leising, G. Tailoring of the color conversion elements in phosphor-converted high-power LEDs by optical simulations. *IEEE Photon. Technol. Lett.* **2008**, *20*, 739–741. [CrossRef]
29. Adachi, S. Photoluminescence properties of Mn 4+-activated oxide phosphors for use in white-LED applications: a review. *J. Lumin.* **2018**, *201*, 263–281. [CrossRef]